

Freezing/Thawing Effects on the Exfoliation of Montmorillonite in Gelatin-Based Bionanocomposite

Changdao Mu,¹ Xinying Li,² Yige Zhao,³ Hanguang Zhang,¹ Liangjie Wang,¹ Defu Li¹

¹Department of Pharmaceutics and Bioengineering, Sichuan University, Chengdu, Sichuan, China

²College of Chemistry and Environment Protection Engineering, Southwest University for Nationalities, Chengdu, Sichuan, China

³Faculty of Engineering, China University of Geosciences, Wuhan, Hubei, China

Correspondence to: D. Li (E-mail: lidifu@scu.edu.cn)

ABSTRACT: Freezing/thawing is used as a new method to elaborate exfoliated gelatin-Montmorillonite (MMT) bionanocomposites. The data of X-ray diffraction and transmission electron microscopy indicate that freezing/thawing is an effective approach to exfoliate the clay for concentrations higher than 5 mass% in gelatin matrix. In addition, after freezing/thawing process to introduce, the crystallinity (triple-helix content) of gelatin-MMT bionanocomposites is improved, revealing that freezing/thawing method has the advantages for gelatin molecules to renature into triple-helix. Specially, the data of Fourier transform infrared indicate that freezing/thawing may induce more hydrogen bond interactions in gelatin-MMT bionanocomposites due to the better dispersion of MMT. The mechanical measurements and thermogravimetric analysis show that gelatin-MMT bionanocomposites prepared by freezing/thawing display enhanced mechanical properties and thermal stability in comparison with the ones prepared by conventional blending at the same clay content. © 2012 Wiley Periodicals, Inc. *J. Appl. Polym. Sci.* 000: 000–000, 2012

KEYWORDS: biopolymers and renewable polymers; clay; composites; mechanical properties; crystallization

Received 4 July 2012; accepted 22 August 2012; published online

DOI: 10.1002/app.38511

INTRODUCTION

Biopolymers-based biodegradable materials have recently received increasing attention, since petroleum-based plastic materials have led to serious environmental concerns, as a result of their nondegradable and nonrenewable nature. In addition, the increasing high oil price is another driving force for the development of substitutes for synthetic plastic.^{1–8} Gelatin is an animal protein obtained by a controlled hydrolysis of the fibrous insoluble collagen present in bones and skin generated as waste during animal slaughtering and processing.⁹ With the merits of low cost, biodegradability, nontoxicity, and renewability, gelatin is suitable for use as raw materials of new environmentally friendly materials.¹⁰ However, the poor mechanical properties and thermal stability of gelatin itself limit its application as structural materials.¹¹ Therefore, many researchers are working at the realm of reinforcement of gelatin.

Clay recently attracted a great deal of attention from materials scientists as a result of its inexpensiveness, chemical and thermal stability, and good mechanical properties. The effect of clay on improving the mechanical and thermal properties of polymer matrix has caused a lot of interest. The combination of nano-sized clay and biopolymer matrix has become an emerging

group of hybrid materials, namely, bionanocomposites.^{8,12–14} Montmorillonite (MMT), one of the most common smectite clays, naturally abundant and toxin-free, is a promising reinforcement material in food, medicine, cosmetic, and healthcare recipients.¹⁵ Specially, gelatin-MMT bionanocomposites are widely studied by many researchers.^{16–20} In Rao's study,¹⁶ transparent gelatin-clay nanocomposites films were made through solution processing, of which mechanical performance and melting point increased distinctly. Zheng and coworkers had done a series of research on gelatin-MMT bionanocomposites. The thermal stability and mechanical properties of the bionanocomposites were significantly improved.^{17–19}

In general, three different types of polymer/clay nanocomposites are achievable, namely intercalated nanocomposites, flocculated nanocomposites, and exfoliated nanocomposites.²¹ Best performances are commonly observed with the exfoliated structures.^{7,16,21,22} To date, many attempts have been made to obtain exfoliated bionanocomposites. Severe stirring and ultrasonic irradiation are the simple methods. However, they play a poor role when the clay content is high.^{7,17,23,24} Ruseckaite and coworkers²⁴ had reported that lower sonication times (10 min) did not allow to exfoliate the clay for concentrations higher

than 5 mass% MMT. Contrary, higher sonication times (30 min) conducted to agglomeration of clay nanoparticles. In the study of Dang et al.,⁸ by adjusting the solution pH value below the isoelectric point of silk fibroin (SF) protein, the SF was in the cation state and it could interact strongly with MMT surface. In this way, novel SF-MMT bionanocomposites with good clay dispersion were successfully obtained. Similarly, the well-exfoliated plasticized starch-based bionanocomposites were successfully elaborated by using cationic starch as a new clay organomodifier to better match the polarity of the matrix and thus to facilitate the clay exfoliation process.⁷ In addition, the replacement of interlayer cations with quarternized ammonium or phosphonium cations, preferably with long alkyl chains, makes MMT easy to disperse into a polymer matrix.²¹ However, organophilic MMT has poor dispersion in hydrophilic biopolymer matrix due to its high organophilic. In our previous study, it was found that the cetyltrimethyl ammonium bromide modified MMT aggregated more in gelatin matrix than MMT, resulting in the poorer effects on improving the mechanical and thermal properties of gelatin bionanocomposites.

The freezing/thawing technique is well applied to produce stable sponges and gels which are physically crosslinked by the presence of hydrogen-bonding interactions and crystalline regions.^{25–28} It has been reported that freezing can enforce phase separation, ice growth, and changes in pH,^{29,30} which shows the potential application in exfoliation of nanoclay in bionanocomposites. However, as far as we know, freezing/thawing has not been used to elaborate exfoliated bionanocomposites. Therefore, we attempt to use freezing/thawing as a new method to prepare exfoliated gelatin-MMT bionanocomposites. In the present work, gelatin-MMT bionanocomposites were prepared with or without freezing/thawing process. The structure and properties of gelatin-MMT bionanocomposites are characterized by X-ray diffraction (XRD), Fourier transform infrared (FTIR), transmission electron microscopy (TEM), mechanical measurements, and thermogravimetric analysis (TGA).

EXPERIMENTAL

Materials

Gelatin type B was purchased from Aladdin Reagent Database, Bloom 250. (Shanghai, China). Sodium MMT was kindly supplied by Zhejiang Fenghong Clay Chemicals (Anji, China). The cationic exchange capacity of MMT was 100 mmol/100 g. Formamide was purchased from Kelong Chemical Reagent Company (Chengdu, China).

Preparation of Gelatin-MMT Bionanocomposites

Gelatin solution (10%, w/v) was prepared by dissolving gelatin powder in distilled water for 30 min and then heated at 60°C for 30 min under continuous stirring. Formamide was added as plasticizer with a concentration of 20 wt % (based on dry gelatin weight). MMT powder was dispersed into distilled water under stirring for 12 h at room temperature to produce a 1% (w/v) solution. Then, certain volume of gelatin and MMT solution was mixed and stirred at 60°C for 1 h. The achieved mixture was divided into two parts: one was poured onto Teflon Petri dishes (9 cm diameters) and conditioned at 25°C for 48 h

to obtain G-MMT bionanocomposites. The samples with 0, 1/100, 2/100, 5/100, and 10/100 MMT contents were named G0, G-1MMT, G-2MMT, G-5MMT, and G-10MMT, respectively. The rest mixture was poured onto Teflon Petri dishes and frozen at -20°C for 24 h. Then, the mixture was subsequently thawed and conditioned at 25°C for 48 h to obtain freezing gelatin-MMT (FG-MMT) bionanocomposites. The samples with 0, 1/100, 2/100, 5/100, and 10/100 MMT contents were named FG0, FG-1MMT, FG-2MMT, FG-5MMT, and FG-10MMT, respectively. All samples were stored in a desiccator at 25°C and 50 ± 3% relative humidity (RH) before measurements.

XRD Analysis

The XRD analysis profiles were obtained using an 18 KW rotating anode X-ray diffractometer (MXPAHF, Japan) with a fixed CuK α radiation of 0.154 nm. The diffraction angle was scanned at a rate of 2°/min. The crystallinity of samples was evaluated by using the following equation³¹

$$\text{Crystallinity} = \frac{A_c}{A_c + A_a} \times 100 \quad (1)$$

where A_c and A_a are the area of crystalline and amorphous diffraction peaks at 2θ scale close to 7.5 and 21.5°, respectively.

TEM Measurement

TEM was used to investigate the nanostructure of gelatin-MMT bionanocomposites. The samples for TEM were prepared by embedding the bionanocomposites in the epoxy resin and microtoming them to 80 nm thick by Leica EMUC6/FC6 ultramicrotomy. TEM measurements were carried out with a FEI Tecnai G² F20 instrument with an acceleration voltage of 200 KV.

FTIR Measurement

FTIR spectra of the samples were obtained from discs containing ~2.0 mg sample in ~20 mg potassium bromide (KBr). The measurements were carried on a Perkin-Elmer Spectrum One FTIR spectrophotometer at the resolution of 4 cm⁻¹ in the wave number region 400–4000 cm⁻¹.

Thermogravimetric Analysis

About 4.0 mg sample was put into Al₂O₃ crucible for the TGA measurement. TGA measurements were performed on a Netzsch TG 209F1 instrument under nitrogen atmosphere to avoid thermo-oxidative reactions. The measurements were running from 40°C up to 800°C at a heating rate of 10°C/min.

Mechanical Tests

Tensile strength (TS) and elongation at break (EB) of the bionanocomposites were determined using a servo control universal testing machine (AI-7000 S, Gotech Testing Machines Inc., Taiwan).⁵ The measurements were made at 25°C and 50% RH in a controlled room. Two rectangular strips (width 5 mm; length 50 mm) were prepared from each sample to determine their mechanical properties. Initial grip separation and mechanical crosshead speed were set at 25 and 100 mm/min, respectively. In each bionanocomposite type, nine samples were tested.

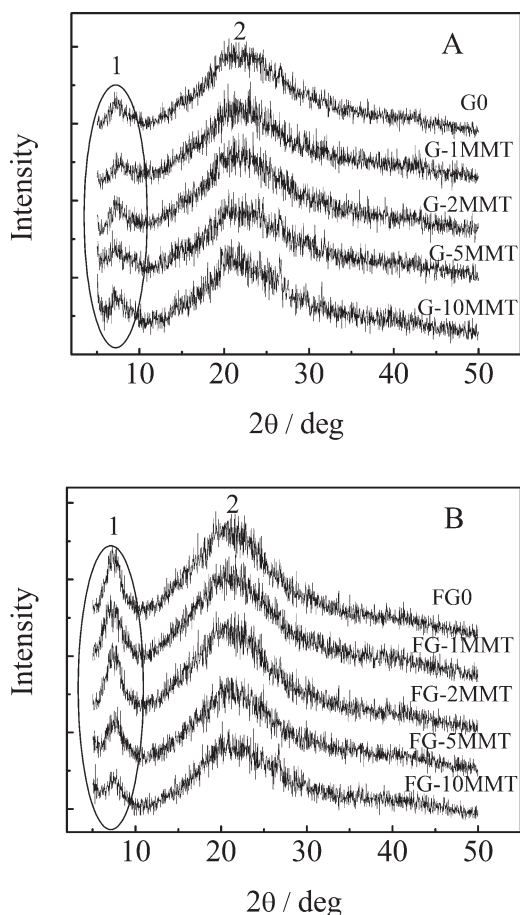


Figure 1. XRD patterns of G-MMT bionanocomposites (A) and FG-MMT bionanocomposites (B) with various MMT contents.

RESULTS AND DISCUSSION

Figure 1 shows the XRD patterns of G-MMT and FG-MMT bionanocomposites with various MMT contents. It is well-known that the partially crystalline gelatin shows a characteristic peak at $2\theta \approx 7-8^\circ$, which is due to the triple-helix structure in

Table I. The Crystallinity of G-MMT and FG-MMT Bionanocomposites with Various MMT Contents

Samples	Crystallinity (%)
G0	4.9 ± 0.12
G-1MMT	4.7 ± 0.17
G-2MMT	4.8 ± 0.18
G-5MMT	4.7 ± 0.21
G-10MMT	4.6 ± 0.13
FG0	12.3 ± 0.15
FG-1MMT	12.1 ± 0.17
FG-2MMT	11.8 ± 0.09
FG-5MMT	9.7 ± 0.11
FG-10MMT	8.3 ± 0.23

collagen and also in renatured gelatin.³² In Figure 1, one relatively sharp peak 1 is observed at $2\theta \approx 7.5^\circ$ and a broad distribution 2 at $2\theta \approx 21.5^\circ$ for both measurements. The peak 1 is assigned to the partially crystalline region originating from the triple-helix structure, whereas the second broad distribution 2 is due to the amorphous fraction of bionanocomposites.^{29,30} Based on this, the crystallinity (triple-helix content) of G-MMT and FG-MMT bionanocomposites with various MMT contents is calculated and presented in Table I. It shows that G0, G-1MMT, G-2MMT, G-5MMT, and G-10MMT have low crystallinity of $\sim 5\%$. The result indicates that gelatin in G-MMT bionanocomposites has low degree of renaturation. It is known that in gelatin-based materials prepared from aqueous solutions by evaporating the solvent off at temperatures above 35°C , gelatin macromolecules assume the conformation of a statistical coil with no indications of ordering. Below 35°C , gelatin macromolecules partially renature into their original collagenlike helical structure.^{33,34} In the present work, G-MMT bionanocomposites were obtained by conditioning the gelatin-MMT mixture at 25°C for 48 h. During this period, low degree of renaturation is attained.

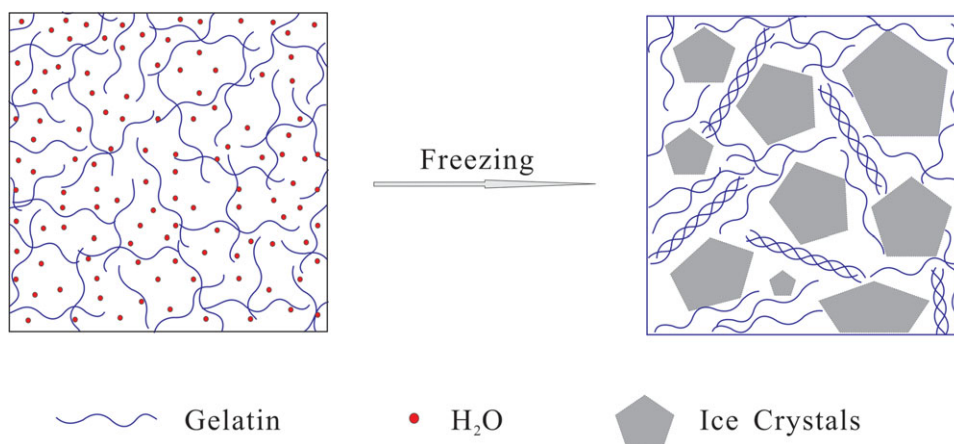


Figure 2. Schematic illustration of renaturation of gelatin during the freezing process. [Color figure can be viewed in the online issue, which is available at wileyonlinelibrary.com.]

Conversely, Table I shows that the crystallinity of FG-MMT bionanocomposites is decreased with the increase of MMT content, indicating the destruction of triple-helical crystalline structure of gelatin molecules by MMT addition. The result is often observed in other nanocomposites systems.¹⁶ However, it is worth noting that the crystallinity of FG0 is raised to 12.3, which is ~ 2.5 times as that of G0, and FG-MMT bionanocomposites both have higher crystallinity than those of G-MMT bionanocomposites at the same MMT loading. The result suggests that freezing/thawing method has the advantages for gelatin molecules to renature into triple-helix. It has been reported that freezing can enforce phase separation and densification, which occurs as the solution freezes and the polymer is rejected from the growing ice crystallites.²⁸ Since densification will result in crystallization. Freezing/thawing possibly increases the crystallinity of FG-MMT bionanocomposites by phase separation with ice crystals formation and subsequent densification, making more gelatin chains packing and renaturing (Figure 2). The same phenomenon has been observed in poly(vinyl alcohol) hydrogels.^{25,35}

Figure 3 shows the low-angle XRD patterns of MMT, G-MMT bionanocomposites, and FG-MMT bionanocomposites. In Figure 3(A), one relatively sharp peak is observed at $2\theta \approx 6.35^\circ$, which is the diffraction peak (d001) of MMT. Note that the diffraction peak (d001) of MMT in G-MMT bionanocomposites [Figure 3(B)] shifts from 6.35 to 4.70° . According to the Bragg's law: $\lambda = 2 d \sin\theta$, the peak shifting from higher diffraction angle to lower diffraction angle is due to increase in the d -spacing, which increases from 1.35 to 1.88 nm. This provides a direct evidence to show that gelatin molecules have been intercalated into the interlayer of MMT in G-MMT bionanocomposites.^{15,36} Furthermore, Figure 3(B) shows that the intensity of peak (d001) in G-1MMT is very low, whereas it is raised to higher level in G-2MMT, G-5MMT, and G-10MMT. The low-peak intensity observed for G-1MMT is caused by the low MMT concentration, and an increase in this diffraction peak intensity is due to the increase in MMT concentration.²⁴ In addition, the clay layers are usually exfoliated when the clay content of nanocomposites is much low.²¹ Some exfoliation structures in G-1MMT should be formed, which will also decrease the peak (d001) intensity.

Figure 3(C) shows the low-angle XRD patterns of FG-MMT bionanocomposites. It is noteworthy that the low-angle XRD patterns of FG-MMT bionanocomposites change dramatically in comparison with G-MMT bionanocomposites. The diffraction peak (d001) in FG-1MMT, FG-2MMT, and FG-5MMT is disappeared, whereas it is very low in FG-10MMT at $2\theta \approx 4.70^\circ$. The absence of diffraction peak (d001) in FG-1MMT, FG-2MMT, and FG-5MMT indicates the formation of exfoliation structure. Intensity decrease of diffraction peak (d001) in FG-10MMT indicates the transition of intercalated structures to exfoliated ones. Moreover, the low intensity of diffraction peak (d001) reveals that the exfoliation plays a dominant role in FG-10MMT with high MMT loading. Severe stirring and ultrasonic irradiation techniques have been used to obtain exfoliated structures of bionanocomposites. However, they play a poor role when the MMT content is high.^{17,24} Ruseckaite and coworkers²⁴ reported

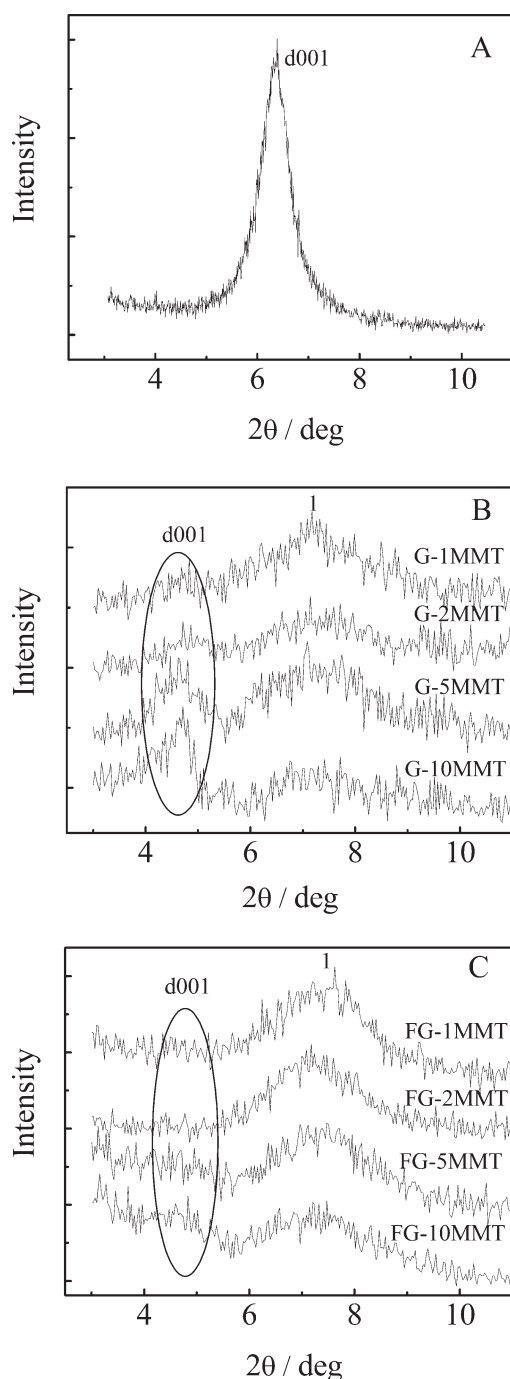


Figure 3. Low-angle XRD patterns of MMT (A), G-MMT bionanocomposites (B) and FG-MMT bionanocomposites (C).

that lower sonication times (10 min) did not allow to exfoliate clay for concentrations higher than 5 mass% MMT. Contrary, higher sonication times (30 min) conducted to agglomeration of clay nanoparticles. By this token, freezing/thawing is an effective mean to prepare exfoliated gelatin-MMT bionanocomposites. Conversely, freezing and thawing of MMT in pure water had been studied with time-resolved synchrotron XRD. It was found that d001 diffraction ring moved further from the centre (shifting to higher diffraction angle) at -15 and -50°C ,

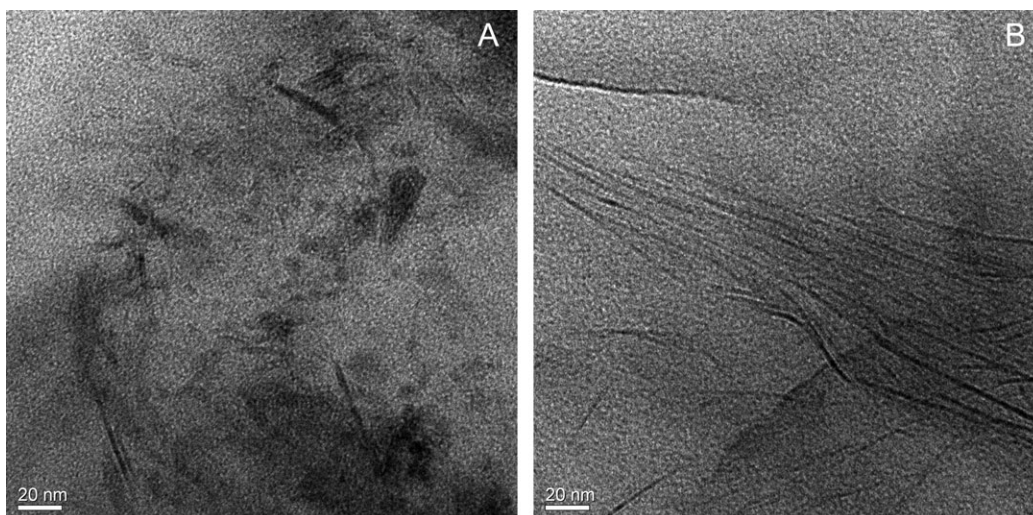


Figure 4. TEM micrographs of G-2MMT (A) and FG-2MMT (B).

indicating dehydration of MMT.³⁷ The result indicates that freezing/thawing can not induce exfoliation of pure MMT. From this, during the freezing/thawing process, the intercalated MMT by gelatin molecules may be a prerequisite for exfoliation.

To further investigate the dispersion and morphology of MMT in gelatin-MMT bionanocomposites, TEM measurement was applied. The TEM micrographs of G-2MMT and FG-2MMT are shown in Figure 4. It can be seen from Figure 4(A) that a large amount of MMT is stacked together in G-2MMT while a few exfoliated single clay platelets are observed. However, Figure 4(B) shows that MMT layers in FG-2MMT are well exfoliated (the dark lines are the MMT layers). Overall, the TEM results show much better MMT dispersion in FG-2MMT than G-2MMT. The TEM observations agree well with the above XRD results. On the basis of XRD patterns and TEM micrographs, gelatin-MMT nanocomposites with good clay dispersion were successfully prepared via freezing/thawing method.

To sum up, the gelatin-MMT bionanocomposites prepared by conventional blending will have intercalated structures accompanied with exfoliated ones. After freezing/thawing process to introduce, the gelatin-MMT bionanocomposites present two changes (Figure 5): one is that the crystallinity (triple-helix content) of gelatin-MMT bionanocomposites is improved, revealing that freezing/thawing method has the advantages for gelatin molecules to renature into triple-helix. The other one is that MMT in gelatin-MMT bionanocomposites is well exfoliated, suggesting that freezing/thawing is an effective mean to prepare exfoliated gelatin-MMT bionanocomposites. However, during the freezing/thawing process, the intercalated MMT by gelatin molecules may be a prerequisite for exfoliation.

Figure 6 shows the FTIR spectra for G0, G-1MMT, G-10MMT, FG0, FG-1MMT, and FG-10MMT. The bands ~ 3440 , ~ 2930 , 1636 – 1661 , and 1549 – 1558 cm^{-1} are denoted as A, B, I, and II amide bands, respectively. Generally, the amide A and B bands

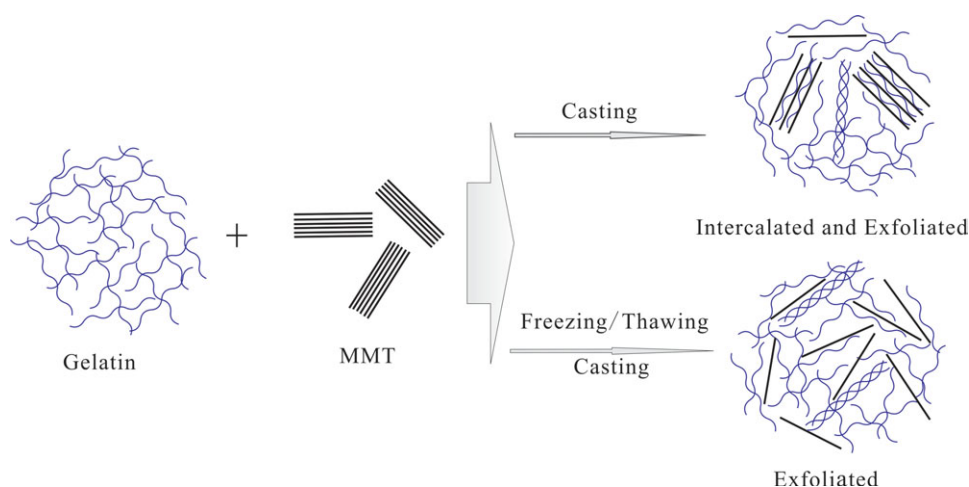


Figure 5. Schematic illustration of fabricating gelatin-MMT bionanocomposites with and without freezing/thawing process. [Color figure can be viewed in the online issue, which is available at wileyonlinelibrary.com.]

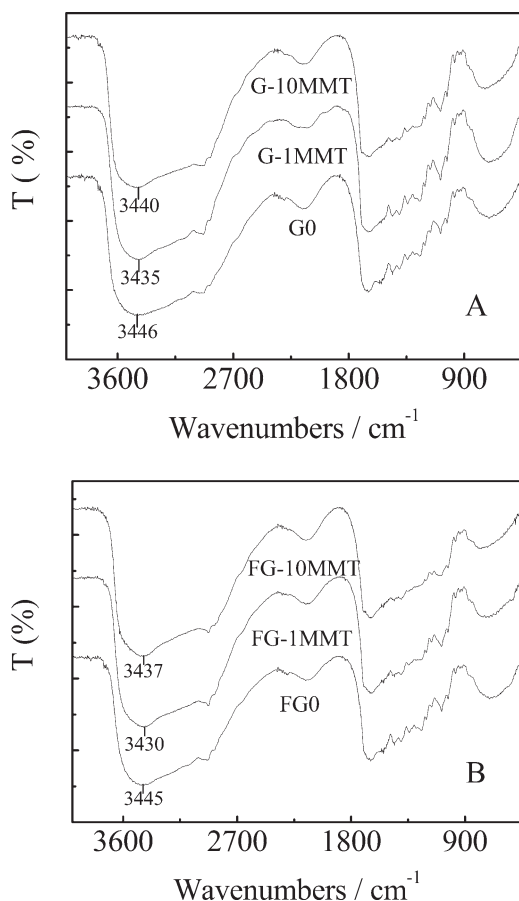


Figure 6. FTIR spectra for G0, G-1MMT, G-10MMT, FG0, FG-1MMT and FG-10MMT.

are mainly associated with the stretching vibrations of N—H groups. The amide I band is originated from C=O stretching vibrations coupled to N—H bending vibration. The amide II band arises from the N—H bending vibrations coupled to C—N stretching vibrations.³⁸ Figure 6(A) shows that the positions of B, I, and II amide bands in G-1MMT and G-10MMT are nearly unchanged while the amide A shifts to low-frequency shoulder in comparison with G0. Commonly, there are strong electrostatic interactions between MMT and protein and hydrogen bond interactions between carbonyl groups in protein and hydroxyl groups within clay galleries.^{21–24,39–41} Changed position of amide A band in Figure 6(A) indicates the hydrogen bond interactions between gelatin and MMT. Note that amide A in G-1MMT shifts to lower frequency than that in G-10MMT. It suggests that the better dispersion of MMT in G-1MMT may promote more hydrogen bond interactions formation. The same results can be obtained in FG-MMT bionanocomposites. However, Figure 6 shows that amide A in FG-MMT bionanocomposites shifts to lower frequency than that in G-MMT bionanocomposites with the same MMT content, indicating more hydrogen bond interactions formation in FG-MMT bionanocomposites. MMT is well exfoliated in FG-MMT bionanocomposites while the intercalated and exfoliated structures are accompanied in G-MMT bionanocomposites, which maybe

induce more hydrogen bond interactions in FG-MMT bionanocomposites.

Table II shows the TS and EB of G-MMT and FG-MMT bionanocomposites. It can be seen that the addition of MMT can greatly improve the mechanical properties of G-MMT bionanocomposites. G-1MMT with 1/100 clay content exhibits a TS of 3.19 MPa and an EB of 46.02%. When MMT content reaches 5/100 (G-5MMT), the TS is raised to 3.80 MPa, which is 1.7 times as that of G0. The increase of MMT causes TS to increase and EB to decrease, suggesting the occurrence of physical cross-linking between gelatin and MMT. However, as the MMT content is over 5/100, the TS begins to decrease. The results arise from the poor dispersion of clay and the aggregation of gelatin chains induced by excess clay addition, which had been reported and well explained in previous works.¹⁷ The same phenomenon is observed in FG-MMT bionanocomposites. However, Table II shows that the FG0 exhibits a TS of 13.22 MPa, which is 5.9 times as that of G0. Crystallinity is a factor to impact polymer's TS, which generally enhances a polymer's modulus. It has been reported that the gelatin with high crystallinity (triple-helix content) was stronger.^{33,34} Hence, the higher crystallinity of FG0 gives higher TS. Furthermore, Table II shows that the TS of FG-MMT bionanocomposites is both higher than that of G-MMT bionanocomposites with the same MMT content. The high crystallinity of FG-MMT bionanocomposites should be one of the contributors to induce high TS. An additional factor to impact TS is the dispersion of MMT. Best performances are commonly observed with the exfoliated structures. So, the well-exfoliated structure of FG-MMT bionanocomposites should be another one of the contributors to induce high TS.

Figure 7 shows the TGA curves of G-MMT bionanocomposites and FG-MMT bionanocomposites with various MMT contents. Thermal decomposition of bionanocomposites is a gradual process with three main stages in the TGA curves. The first one, in the range of 80–250°C, is assigned to the loss of low-molecular mass compounds, mainly adsorbed and bounded water. The second and main stage, in the range of 250–500°C, is mainly related to the degradation of gelatin chains. The higher temperature step which exceeds 510°C can be attributed to the decomposition of more thermally stable structure.²⁴ The residues at

Table II. Tensile Strength and Elongation at Break of G-MMT and FG-MMT Bionanocomposites

Samples	TS (MPa)	EB (%)
G0	2.22 ± 0.57	49.06 ± 3.62
G-1MMT	3.19 ± 0.21	46.02 ± 5.33
G-2MMT	3.31 ± 0.31	43.93 ± 2.78
G-5MMT	3.80 ± 0.26	42.18 ± 4.12
G-10MMT	3.02 ± 0.52	34.55 ± 2.70
FG0	13.22 ± 0.52	15.99 ± 1.05
FG-1MMT	20.90 ± 1.01	15.24 ± 1.12
FG-2MMT	22.08 ± 0.89	14.23 ± 2.30
FG-5MMT	23.91 ± 0.79	11.96 ± 1.62
FG-10MMT	20.35 ± 1.04	10.37 ± 2.00

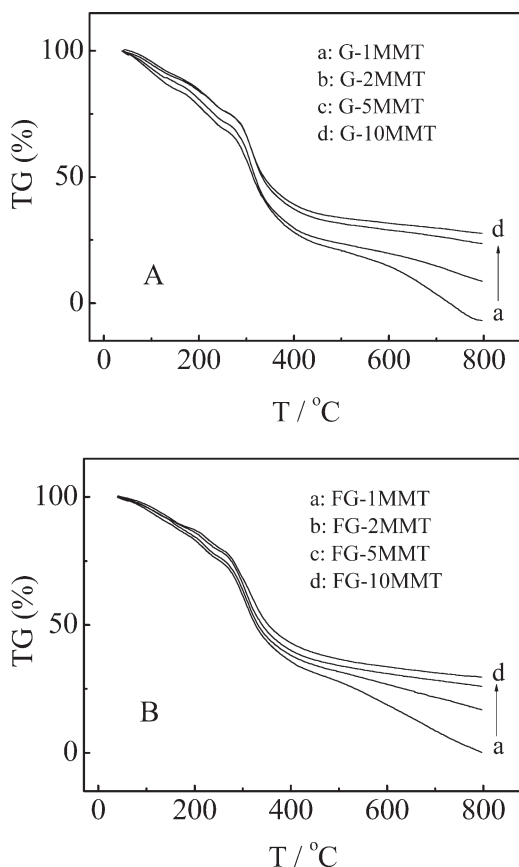


Figure 7. TGA curves of G-MMT bionanocomposites (A) and FG-MMT bionanocomposites (B) with various MMT contents.

250, 500, and 700°C of the thermal degradation of G-MMT and FG-MMT bionanocomposites are given in Table III. The results show that the addition of MMT produces a delay in mass loss in the temperature range of gelatin chains degradation (250–500°C). It is known that gelatin has a good electrostatic interaction and can further form hydrogen bond interactions with clay. MMT act as physical crosslinker between gelatin molecules result in the thermal improvement of gelatin-MMT bionanocomposites. In addition, the incorporation of clay into the

Table III. Residue at 250°C, 500°C, and 700°C of the Thermal Degradation of G-MMT Bionanocomposites and FG-MMT Bionanocomposites

Samples	Residue at 250°C (%)	Residue at 500°C (%)	Residue at 700°C (%)
G-1MMT	69.2	20.9	3.5
G-2MMT	72.1	23.9	14.8
G-5MMT	76.4	31.4	26.8
G-10MMT	76.4	33.9	29.4
FG-1MMT	75.2	27.9	8.9
FG-2MMT	76.7	31.7	21.8
FG-5MMT	79.0	34.2	28.4
FG-10MMT	80.2	36.8	31.5

gelatin matrix is found to enhance thermal stability by acting as a superior insulator and mass transport barrier during decomposition.¹⁶ Note that the FG-MMT bionanocomposites have higher residue than that of G-MMT bionanocomposites with the same MMT content at 250, 500, and 700°C. Agglomerated clay particles do not significantly affect the thermal stability of the polymer matrix.⁴² The well-exfoliated structure of FG-MMT bionanocomposites should be the contributors to induce high thermal stability.

CONCLUSIONS

In the present work, freezing/thawing is used as a new method to elaborate exfoliated gelatin-MMT bionanocomposites. The effects of freezing/thawing on the structure and properties of gelatin-MMT bionanocomposites are studied. The results show that after freezing/thawing process to introduce, the gelatin-MMT bionanocomposites present two changes: one is that the crystallinity (triple-helix content) of gelatin-MMT bionanocomposites is improved, revealing that freezing/thawing method has the advantages for gelatin molecules to renature into triple-helix by phase separation and subsequent densification. The other one is that MMT in gelatin-MMT bionanocomposites is well exfoliated, suggesting that freezing/thawing is an effective mean to prepare exfoliated gelatin-MMT bionanocomposites. As a consequence, the well-exfoliated gelatin-MMT bionanocomposites prepared by freezing/thawing display enhanced mechanical properties and thermal stability in comparison with the ones prepared by conventional blending at the same clay content.

ACKNOWLEDGMENTS

This work was supported by National Natural Science Foundation of China, grant 21206098; Program for Changjiang Scholars and Innovative Research Team in University, grant IRT1163; and Science and Technology Planning Project of Sichuan Province; grant 2011HH0008.

REFERENCES

- Pojanavaraphan, T.; Magaraphan, R.; Chiou, B.; Schiraldi, D. A. *Biomacromolecules* **2010**, *11*, 2640.
- Wu, T. M.; Wu, C. Y. *Polym. Degrad. Stab.* **2006**, *91*, 2198.
- Bordes, P.; Pollet, E.; Avérous, L. *Prog. Polym. Sci.* **2009**, *34*, 125.
- Xie, Y.; Kohls, D.; Noda, I.; Schaefer, D. W.; Akpalu, Y. A. *Polymer* **2009**, *50*, 4656.
- Mu, C. D.; Guo, J. M.; Li, X. Y.; Lin, W.; Li, D. F. *Food Hydrocolloid* **2012**, *27*, 22.
- Sothornvit, R.; Hong, S. I.; An, D. J.; Rhim, J. W. *LWT-Food Sci. Technol.* **2010**, *43*, 279.
- Chivrac, F.; Pollet, E.; Schmutz, M.; Avérous, L. *Biomacromolecules* **2008**, *9*, 896.
- Dang, Q. Q.; Lu, S. D.; Yu, S.; Sun, P. C.; Yuan, Z. *Biomacromolecules* **2010**, *11*, 1796.
- Patil, R. D.; Mark, J. E.; Apostolov, A.; Vassileva, E.; Fakirov, S. *Eur. Polym. J.* **2000**, *36*, 1055.

10. Carvalho, R. A.; Sobral, P. J. A.; Thomazine, M.; Habitante, A. M. Q. B.; Giménez, B.; Gómez-Guillén, M. C.; Montero, P. *Food Hydrocolloid* **2008**, *22*, 1117.
11. Bigi, A.; Cojazzi, G.; Panzavolta, S.; Roveri, N.; Rubini, K. *Biomaterials* **2002**, *23*, 4827.
12. Avinash, J. P.; Muthusamy, E.; Mann, S. *J. Mater. Chem.* **2005**, *15*, 3838.
13. Huang, X. S.; Netravali, A. N. *Biomacromolecules* **2006**, *7*, 2783.
14. Lin, J. J.; Wei, J. C.; Tsai, W. C. *J. Phys. Chem. B* **2007**, *111*, 10275.
15. Park, H. M.; Li, X. C.; Jin, C. Z.; Park, C. Y.; Cho, W. J.; Ha, C. S. *Macromol. Mater. Eng.* **2002**, *287*, 553.
16. Rao, Y. Q. *Polymer* **2007**, *48*, 5369.
17. Zheng, J. P.; Li, P.; Ma, Y. L.; Yao, K. D. *J. Appl. Polym. Sci.* **2002**, *86*, 1189.
18. Li, P.; Zheng, J. P.; Ma, Y. L.; Yao, K. D. *J. Appl. Polym. Sci.* **2003**, *88*, 322.
19. Zheng, J. P.; Li, P.; Yao, K. D. *J. Mater. Sci. Lett.* **2002**, *21*, 779.
20. Chiellini, E.; Cinelli, P.; Fernandes, E. G.; Kenawy, E. S.; Lazzeri, A. *Biomacromolecules* **2001**, *2*, 806.
21. Ray, S. S.; Okamoto, M. *Prog. Polym. Sci.* **2003**, *28*, 15391.
22. Vaia, R. A.; Giannelis, E. P. *Macromolecules* **1997**, *30*, 8000.
23. Zhang, L. N.; Chen, P. *Biomacromolecules* **2006**, *7*, 1700.
24. Martucci, J. F.; Vázquez, A.; Ruseckaite, R. A. *J. Therm. Anal. Calorim.* **2007**, *89*, 117.
25. Hassan, C. M.; Peppas, N. A. *Macromolecules* **2000**, *33*, 2472.
26. Arunyanart, T.; Charoenrein, S. *Carbohydr. Polym.* **2008**, *74*, 514.
27. Mu, C. D.; Liu, F.; Cheng, Q. S.; Li, H. L.; Wu, B.; Zhang, G. Z.; Lin, W. *Macromol. Mater. Eng.* **2010**, *295*, 100.
28. Abitbol, T.; Johnstone, T.; Quinn, T. M.; Gray, D. G. *Soft Matter* **2011**, *7*, 2373.
29. Kumar, A.; Mishra, R.; Reinwald, Y.; Bhat, S. *Mater. Today* **2010**, *13*, 42.
30. Wang, Y. X.; Zhang, C. Y.; Zhang, L. N. *Macromol. Mater. Eng.* **2010**, *295*, 137.
31. Khanna, N. D.; Kaur, I.; Bhalla, T. C.; Gautam, N. *J. Appl. Polym. Sci.* **2010**, *118*, 1476.
32. Ghoshal, S.; Mattea, C.; Denner, P.; Stapf, S. *J. Phys. Chem. B* **2010**, *114*, 16356.
33. Kozlov, P. V. *Polymer* **1983**, *24*, 651.
34. Payne, J. A.; McCormick, A. V.; Francis, L. F. *J. Appl. Polym. Sci.* **1999**, *73*, 553.
35. Lee, M.; Bae, H.; Lee, S.; Chung, N.; Lee, H.; Choi, S.; Hwang, S.; Lee, J. *Macromol. Res.* **2011**, *19*, 130.
36. Park, H. M.; Lee, W. K.; Park, C. Y.; Cho, W. J.; Ha, C. S. *J. Mater. Sci.* **2003**, *38*, 909.
37. Svensson, P. D.; Hansen, S. *Appl. Clay Sci.* **2010**, *49*, 127.
38. Li, D. F.; Mu, C. D.; Cai, S. M.; Lin, W. *Ultrason. Sonochem.* **2009**, *16*, 605.
39. Alexandre, M.; Dubois, P. *Mater. Sci. Eng.* **2000**, *28*, 1.
40. Kawasumi, M.; Hasegawa, N.; Kato, M.; Usuki, A.; Okada, A. *Macromolecules* **1997**, *30*, 6333.
41. Lee, S. R.; Park, H. M.; Lim, H.; Kang, T.; Li, X.; Cho, W.; Ha, C. S. *Polymer* **2002**, *43*, 2495.
42. Pramoda, K. P.; Liu, T. X.; Liu, Z. H.; He, C. B.; Sue, H. *J. Polym. Degrad. Stab.* **2003**, *81*, 47.